arXiv:1410.1244v2 [cond-mat.supr-con] 26 Nov 2014

Anomalous scaling of the specific-heat jump ΔC vs. T_c in the Fe-based superconductors: the $\pm$S-wave pairing state model

Yunkyu Bang[1] and G. R. Stewart[2]
[1]*Department of Physics, Chonnam National University, Kwangju 500-757, Republic of Korea*
[2] *Physics Department, University of Florida, Gainesville, FL 32611-8440, USA*
(Dated: December 1, 2014)

The strong power law behavior of the specific heat jump ΔC vs. T_c ($\Delta C/T_c \sim T_c^{\alpha}, \alpha \approx 2$), first observed by Bud'ko, Ni, and Canfield (BNC)[1], has been confirmed with several families of the Fe-based superconducting compounds with doping. We show here that this anomalous non-BCS behavior is an intrinsic property of the multiband superconducting state paired by a dominant interband interaction ($V_{inter} > V_{intra}$) reflecting the relation $\frac{\Delta_h}{\Delta_e} \sim \sqrt{\frac{N_e}{N_h}}$ near T_c, as in the $\pm$S-wave pairing state. Then this ΔC vs. T_c relation can continuously change from the ideal BNC scaling to a considerable deviation at lower T_c with a moderate variation of the impurity scattering rate.

PACS numbers: 74.20.-z,74.20.Rp,74.70.Xa

Introduction. — The specific heat (SH) jump ΔC is the most well known thermodynamic signature of the second order phase transition and hence contains the generic information of the transition as well as the material specific information. For example, the BCS theory of superconductivity predicts the universal ratio $\Delta C/C_{el}|_{T=T_c} = 1.43$, hence $\Delta C/T_c = 1.43\gamma$ is a temperature independent constant and tells us the material specific quantity γ, the Sommerfeld coefficient of the normal state $\gamma = C_{el,n}/T$. In view of this BCS prediction, $\Delta C/T_c = const.$, the experimental observation by Bud'ko, Ni, and Canfield (BNC)[1], $\Delta C/T_c \approx T_c^2$ for a family of doped Ba($Fe_{1-x}TM_x$)$_2As_2$ compounds with TM=Co, Ni is a very intriguing behavior and stimulated active investigations both experimentally and theoretically. After the work of Ref.[1], this so-called BNC scaling relation was expanded with an increasing list of the iron pnictide and iron chalcogenide (FePn/Ch) superconducting (SC) compounds[2–9], hence strengthens the speculation that some generic mechanism must exist behind this unusual scaling behavior. However, the recent observation of a strong deviation from the BNC scaling in a series of K-doped $Ba_{1-x}K_xFe_2A_2$ for $0.7 < x \leq 1$ [10] is confusingly contrasted to the Na-doped $Ba_{1-x}Na_xFe_2A_2$ ($0.1 \leq x \leq 0.9$)[8] which displays an excellent BNC scaling.

For the theoretical investigations, there are three attempted explanations. Kogan[11] argued that strong pair-breaking can cause $\Delta C/T_c \propto T_c^2$. The essence of this theory is a dimensional counting. The free energy difference near T_c, $\Delta F = F_s - F_n$, can be expanded in powers of Δ^2 (Δ: the SC order parameter (OP)). In the BCS theory, $\Delta F \propto -N(0)\frac{\Delta^4}{T_c^2}$ [12]. Using the BCS result of $\Delta^2(T) \sim T_c^2(1 - \frac{T}{T_c})$, we get $\Delta C/T_c \propto \frac{\partial^2 \Delta F}{\partial T^2} \sim N(0)$, the well known BCS prediction. In the case of the strong pair-breaking limit, $\Gamma_\pi \gg T_c$ ($\Gamma_\pi =$ pair-breaking rate), considered by Kogan, $\Delta F \propto -N(0)\frac{\Delta^4}{\Gamma_\pi^2}$ by a dimensional counting. Substituting the same BCS behavior of $\Delta^2(T) \propto T_c^2(1 - \frac{T}{T_c})$, we recover the Kogan's result $\Delta C/T_c \sim N(0)\frac{T_c^2}{\Gamma_\pi^2}$. However, we believe that this result is the consequence of an inconsistent approximation[13]. The theory of Vavilov *et al.*[14] mainly studied the coexistence region with magnetic order M and SC order Δ. It is a plausible theory that the coexisting magnetic order over the SC order can substantially reduce ΔC, hence develops a steep variation of ΔC vs. T_c. However this theory didn't reveal a specific reason as to why $\Delta C/T_c$ follows the BNC scaling $\sim T_c^{\alpha}$ with $\alpha \approx 2$. Finally, Zannen[15] attributed the behavior $\Delta C \propto T_c^3$ to the normal state electronic SH with the scaling form $C_{elec}^n \propto T^3$ due to the critical fluctuations near the quantum critical point (QCP). A problem of this theory is that there is no evidence of $C_{elec}^n \propto T^3$ for a wide doping range of the FePn/Ch superconductors. All three theories mentioned above are single band theories and do not particularly utilize the unique properties of the FePn/Ch superconductors. In this paper, we propose a theory in which the multi-band nature of the FePn/Ch superconductors is the root cause for producing the BNC scaling behavior.

Two Band model for the SH jump ΔC. — For a multi-band superconductor, the SH jump formula is generalized as

$$\Delta C = \sum_{i=h,e} N_i(0)\Big(\frac{-d\Delta_i^2}{dT}\Big)\Big|_{T_c} \qquad (1)$$

where the band index "i" counts the different bands and we specify it as the hole and electron band typical in the Fe-based superconductors. $N_{h,e}$ are the DOSs, and $\Delta_{h,e}$ are the SC OPs of each band. In the one band BCS superconductor, using $\Delta^2(T) \sim T_c^2(1 - \frac{T}{T_c})$, the above equation gives $\Delta C/T_c \propto N(0) = const.$ However, in the case of a multi-band superconductor, Eq.(1) can reveal more information for the pairing mechanism as well as the pairing state.

At present the most widely accepted pairing state in the Fe-based superconductors is the sign-changing S-wave state ($\pm$S-wave) mediated by a dominant interband repulsive interaction ($V_{inter} > V_{intra}$)[16]. The essential physics of this $\pm$S-wave state can be studied with the two coupled gap equations[18]

$$\Delta_h = -\big[V_{hh}N_h\chi_h\big]\Delta_h - \big[V_{he}N_e\chi_e\big]\Delta_e, \qquad (2)$$

$$\Delta_e \;=\; -\big[V_{ee}N_e\chi_e\big]\Delta_e - \big[V_{eh}N_h\chi_h\big]\Delta_h,$$

where the pair susceptibility at T_c is defined as

$$\chi_{h,e}(T_c) = T_c\sum_n \int_{-\Lambda_{hi}}^{\Lambda_{hi}} d\xi \frac{1}{\omega_n^2+\xi^2} \approx \ln\Big[\frac{1.14\Lambda_{hi}}{T_c}\Big], \quad (3)$$

where $\omega_n = \pi T_c(2n+1)$ and Λ_{hi} is a pairing energy cut-off. The pairing potentials V_{ab} $(a,b = h,e)$ are all positive and further simplified in this paper as $V_{he} = V_{eh} = V_{inter}$ and $V_{hh} = V_{ee} = V_{intra}$ without loss of generality.

In the limit $V_{intra}/V_{inter} \to 0$, Eq.(1) can be analytically solved and provides the interesting kinematic constraint relation[17]

$$\frac{\Delta_h}{\Delta_e} \sim \sqrt{\frac{N_e}{N_h}} \quad \text{as } T \to T_c, \quad (4)$$

and the critical temperature is given by

$$T_c \approx 1.14\Lambda_{hi}\exp\big[-1/(V_{inter}\sqrt{N_eN_h})\big]. \quad (5)$$

For further modeling the calculation of the experimental data of ΔC vs. T_c for a Fe-122 compound with a series of doping, we first notice that the undoped parent compound such as $BaFe_2As_2$ is a compensated metal, hence has the same number of electrons and holes, i.e. $n_h = n_e$. Therefore it is a reasonable approximation for our model to take $N_h = N_e$ at no doping and then the doping of holes (K, Na, etc.) or electrons (Co, Ni, etc.) is simulated by varying N_h or N_e while keeping $N_e + N_h = N_{tot} = const.$ For the rest of this paper, it is convenient to use the normalized DOSs as $\bar{N}_{h,e} = N_{h,e}/N_{tot}$ and N_{tot} is combined to define the dimensionless coupling constants as $\bar{V}_{intra/inter} = N_{tot}\cdot V_{intra/inter}$.

Expanding the gap equations Eq.(2) near T_c and using Eq.(4), we obtain $\Delta_{h,e}(T)$ near T_c as

$$\Delta_h^2(T) \;\approx\; \frac{2}{1+N_h/N_e}\Delta_{BCS}^2(T), \quad (6)$$
$$\Delta_e^2(T) \;\approx\; \frac{2}{1+N_e/N_h}\Delta_{BCS}^2(T)$$

with $\Delta_{BCS}^2(T) = \pi^2\frac{8}{7\zeta(3)}T_c^2(1-T/T_c)$. Combining the results of Eq.(4) and (6), Eq.(1) provides

$$\frac{\Delta C}{T_c} \approx 4\times(3.06)^2 N_{tot}\cdot(\bar{N}_h\bar{N}_e). \quad (7)$$

This is our key result. In contrast to the one band BCS superconductor, Eq.(7) clearly shows that $\Delta C/T_c$ can have a strong T_c dependence through $\bar{N}_h\bar{N}_e$ even with a constant N_{tot} (see Eq.(5)). With doping in a given FePn/Ch compound, $\bar{N}_h$ and $\bar{N}_e(=1-\bar{N}_h)$ varies over the range of $[0,1]$ of [19]. As such if $(\bar{N}_h\bar{N}_e) \sim T_c^2$ for some region of $\bar{N}_{h,e}$, we would obtain the BNC scaling.

Having analyzed the ideal case ($V_{intra} = 0$), we numerically study the more realistic cases, including the impurity scattering effect. We solve the coupled gap equations Eq.(2) for $\Delta_{h,e}(T)$ near T_c and directly calculate ΔC using Eq.(1). We find that the kinematic constraint of the two band pairing model discovered above is robust. However in order to explain the ideal BNC scaling $\Delta C/T_c \propto T_c^2$ in $Ba(Fe_{1-x}TM_x)_2A_2$ (TM=Co,Ni) as well as its strong deviation in $Ba_{1-x}K_xFe_2A_2$[10], we find that the non-pair-breaking impurity scattering plays a crucial role.

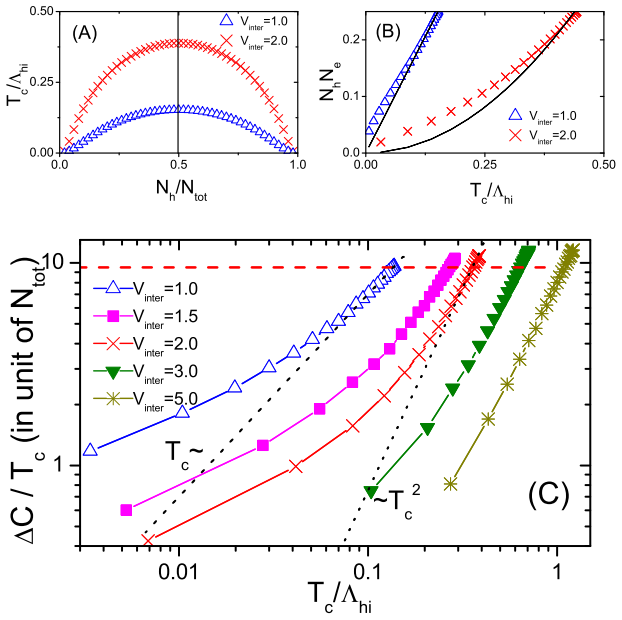

FIG. 1: (Color online) (A) Numerical calculations of T_c vs. $\bar{N}_h$ of the two band model for $\bar{V}_{inter} = 1.0$, and 2.0, respectively, with $\bar{V}_{intra} = 0.0$ for both cases. (B) Plots of $\bar{N}_h\bar{N}_e$ vs. T_c with the same data of (A). Solid lines are of $\sim T_c$ and $\sim T_c^2$, respectively. (C) Numerical calculations of $\Delta C/T_c$ vs. T_c for $\bar{V}_{inter} = 1.0, 1.5, 2.0,$ and 3.0, respectively, with $\bar{V}_{intra} = 0.0$ for all cases. Horizontal dashed line is the BCS limit of $9.36N_{tot}$ and the dotted lines of $\sim T_c$ and $\sim T_c^2$ (BNC scaling) are guides for the eyes.

Numerical results.— In Fig.1(A), we calculated T_c vs. $\bar{N}_h$ of the two band model Eq.(2) for $\bar{V}_{inter} = 1.0$ and 2.0, respectively, with $\bar{V}_{intra} = 0$ for both cases. Indeed, the calculated T_c shows a strong dependence on $\bar{N}_h$, symmetric with respect to $\bar{N}_h = 0.5$ because $\bar{N}_h + \bar{N}_e = 1$. We plot the same data as $\bar{N}_h\cdot\bar{N}_e$ vs. T_c in Fig.1(B). In the case of $\bar{V}_{inter} = 2.0$, we find $\bar{N}_h\cdot\bar{N}_e \sim T_c^2$ near the maximum T_c region which is the necessary condition for the BNC scaling from Eq.(7). It also shows that the overall power of the relation $\bar{N}_h\cdot\bar{N}_e \sim T_c^\alpha$ becomes weaker with the weaker pairing potential $\bar{V}_{inter}$.

Now we calculate $\Delta C(\bar{N}_h)$ from Eq.(1) and Eq.(2), and $\Delta C(\bar{N}_h)$ and $T_c(\bar{N}_h)$ are implicitly related through $\bar{N}_h \in [0,1]$. In Fig.1(C), we plot $\Delta C/T_c$ vs. T_c in log-log scale, for different pairing potentials $\bar{V}_{inter} = 1.0, 1.5, 2.0$ and 3.0, respectively, with $\bar{V}_{intra} = 0.0$ for all cases. As hinted from Fig.1(B), we can see the trend that the region of the BNC scaling $\Delta C/T_c \sim T_c^2$ becomes widened near the maximum T_c region with increasing the pairing potential strength $\bar{V}_{inter}$. With extensive numerical experiments, we found: (1) $\Delta C/T_c$ can become $\sim T_c^2$ for the whole region if $\bar{V}_{inter} > 5.0$, but

this strength of pairing potential is unrealistically large. (2) Including $V_{intra} \neq 0.0$ does not change the general behavior shown in Fig.1(C) as long as $\bar{V}_{intra} < \bar{V}_{inter}/2$.

While we have found that the BNC scaling can be realized in a region near the maximum T_c with the generic two band model, we still need an extra mechanism to enhance the BNC scaling for the wider region of T_c. As shown in Fig.1(A) and Fig.1(B), T_c is maximum when $\bar{N}_e = \bar{N}_h = 0.5$ and it quickly decreases with doping as $\bar{N}_h\bar{N}_e \ll 0.25$ and accordingly one of the OPs, either Δ_h or Δ_e, becomes tiny. Hence, the effect of impurity scattering on the tiny gap becomes increasingly stronger for the lower T_c region where the ratio $\bar{N}_e/\bar{N}_h$ is far from 1. We found that this doping-dependent, therefore T_c-dependent, impurity effect changes the generic $\Delta C/T_c$ vs. T_c relation to a steeper relation at the lower T_c region, hence enhances the region of the BNC scaling even with a moderate strength of $\bar{V}_{inter}$.

Phenomenologically we introduce two parameters of the impurity scattering in the two band model: Γ_0 (intra-band scattering) and Γ_π (inter-band scattering). As we assumed the $\pm S$-wave state, Γ_π causes strong pair-breaking effect (e.g. suppression of T_c and reduction of $\Delta_{h,e}$), but Γ_0 doesn't affect the superconductivity itself[20]. However, the quasiparticle broadening is governed by the sum $\Gamma_{tot} = \Gamma_0 + \Gamma_\pi$ and the calculations of ΔC from Eq.(1) should be generalized with this broadening of the quasiparticle spectra as follows[21],

$$\Delta C = \sum_{i=h,e} N_i \Big(\frac{-d\Delta_i^2}{dT}\Big)\Big|_{T_c} \int_0^\infty \frac{dx}{2}\Big[\frac{1}{\cosh^2(\frac{x}{2})}\Big]\frac{x^2}{x^2 + (\frac{\Gamma_{tot}}{T_c})^2} \quad (8)$$

where $x = \omega/T_c$. The standard pair-breaking effect of Γ_π still enters the pair-susceptibility $\chi_{h,e}(T_c) = T_c \sum_n \int_{-\Lambda_{hi}}^{\Lambda_{hi}} d\xi \frac{1}{\tilde{\omega}_n^2+\xi^2}$ instead of Eq.(3) with $\tilde{\omega}_n = \omega_n + \Gamma_\pi$, therefore Γ_π directly affects T_c and $\left(\frac{-d\Delta_i^2}{dT}\right)$ in Eq.(8). However, increasing Γ_π only[11] doesn't help for producing the BNC scaling as discussed in the Introduction[13]. On the other hand, Eq.(8) above shows that the total quasiparticle damping rate Γ_{tot} entering the thermodynamic average part in Eq.(8) is more important to determine ΔC vs. T_c.

In Fig.2, we show the numerical results of $\Delta C/T_c$ vs. T_c in log-log scale with a choice of a moderate strength of the pairing potentials, $\bar{V}_{inter} = 2.0$ and $\bar{V}_{intra} = 0.5$, and varied the impurity scattering rates Γ_0, and Γ_π. Without impurity scattering (red " $\times$ " symbols, $\Gamma_0 = \Gamma_\pi = 0$), $\Delta C/T_c$ shows the T_c^2 scaling only for the limited region near the maximum T_c and it quickly becomes flattened and slower than $\sim T_c$. Interestingly, this behavior looks very similar to the experimental data of $Ba_{1-x}K_xFe_2A_2$ [10]. Therefore, we speculate that the K-doping in $Ba_{1-x}K_xFe_2A_2$ doesn't introduce many impurity scatterers. Next, only a small increase of impurities (green " + " symbols, $\Gamma_0 = \Gamma_\pi = 0.02$ in unit of Λ_{hi}) immediately changes $\Delta C/T_c$ closer to $\sim T_c^2$ over the whole T_c range, and the case with $\Gamma_0 = 0.1$ and $\Gamma_\pi = 0.05$ (pink " $\diamond$ " symbols) displays an ideal BNC scaling $\Delta C/T_c \sim T_c^2$ for the

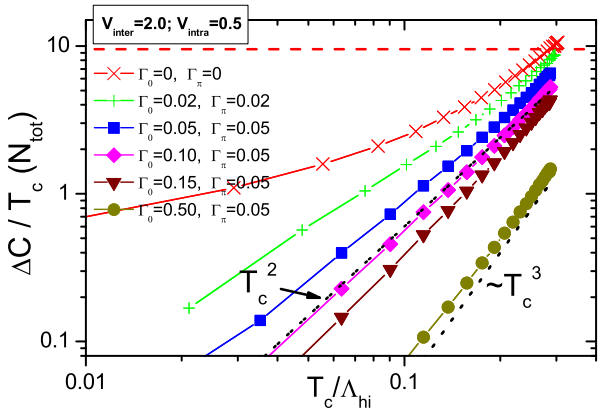

FIG. 2: (Color online) Numerical calculations of $\Delta C/T_c$ vs. T_c with $\bar{V}_{inter} = 2.0$ and $\bar{V}_{intra} = 0.5$, for different impurity scattering strengths of Γ_0 and Γ_π (in unit of Λ_{hi}). Horizontal dashed line is the BCS limit of $9.36N_{tot}$ and the dotted lines of $\sim T_c^2$ (BNC scaling) and $\sim T_c^3$ (super-strong scaling) are guides for the eyes.

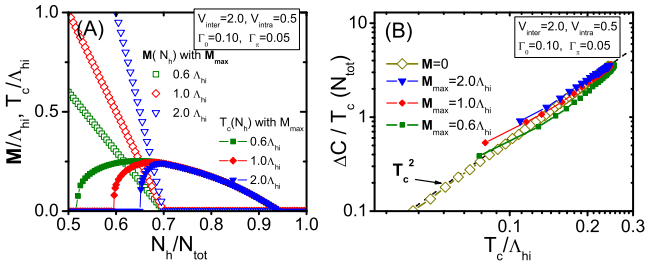

FIG. 3: (Color online) (A) Numerical calculations of T_c vs. $\bar{N}_h$ with coexisting magnetic order $M(\bar{N}_h)$ of three different strengths of $M_{max} = M(\bar{N}_h = 0.5)$=0.6 (blue ∇), 1.0 (red $\diamondsuit$), and 2.0 (green box symbols) (in unit of Λ_{hi}). The pairing interactions and the impurity scattering rates are chosen $\bar{V}_{inter} = 2.0$, $\bar{V}_{intra} = 0.5$, and $\Gamma_0 = 0.10$, $\Gamma_\pi = 0.05$, respectively. (B) Calculated $\Delta C/T_c$ vs. T_c for the corresponding three cases of (A). The calculations of the region ($\bar{N}_h \in [0.7, 1]$) where $M(\bar{N}_h) = 0$ are all the same and displayed with dark yellow "$\diamondsuit$" symbols.

entire range of T_c. Finally, for demonstration purposes, we also show the case with unrealistically large impurity scattering rates, $\Gamma_0 = 0.5$ and $\Gamma_\pi = 0.05$ (dark green " $\circ$ " symbols), which displays $\Delta C/T_c \sim T_c^3$, a super-strong scaling.

Coexistence region with magnetic and SC orders. — Experiments showed that the BNC scaling continues to be valid even when the spin density wave (SDW) order coexists with the SC order in the underdoped regime. Now we would like to extend our model including the magnetic order in the underdoped regime. We took a simple phenomenological approach ignoring the self-consistence between two OPs. We consider only the hole doped region $\bar{N}_h \in [0.5, 1]$, because our model is symmetric with the hole and electron doping. We arbitrarily chose the coexistence region for $0.5 \leq \bar{N}_h < 0.7$, just for the sake of demonstration, and then we introduced the magnetic order $M(\bar{N}_h)$ for this region. The magnetic OP $M(\bar{N}_h)$ linearly grows from zero at $\bar{N}_h = 0.7$ to a

maximum value M_{max} at $\bar{N}_h = 0.5$ as shown in Fig.3(A). When a finite M exists, it affects the superconductivity in two important ways: (1) it weakens the SC pair susceptibility and we take the simplest approximation as $\chi_{h,e}(T_c) = T_c \sum_n \int_0^{\Lambda_{hi}} d\xi \frac{2}{\tilde{\omega}_n^2+\xi^2+M^2}$ [14]. (2) The presence of SDW order M also removes a part of the FSs. Phenomenologically, we mimic this effect by linearly reducing the total DOS N_{tot} starting from $\bar{N}_h = 0.7$ to a maximum reduction at $\bar{N}_h = 0.5$ as $N_{tot}(\bar{N}_h) = N^0_{tot}[1 - a\frac{M(\bar{N}_h)}{\Lambda_{hi}}]$ ($a = 0.5$ was chosen for calculations in Fig.3). With these phenomenological Ansätze, we solved the T_c-equations from Eq.(2) with fixed pairing interactions and damping ($\bar{V}_{inter} = 2.0, \bar{V}_{intra} = 0.5$; and $\Gamma_0 = 0.10, \Gamma_\pi = 0.05$) for three different strengths of M_{max} in Fig.3(A). The results qualitatively simulate the experimental phase diagram: T_c starts decreasing when $M(\bar{N}_h)$ starts developing from $\bar{N}_h = 0.7$ and the reduction of T_c is faster with larger magnetic order.

In Fig.3(B), $\Delta C/T_c$ vs. T_c is calculated for the corresponding three cases of Fig.3(A). The case of $M = 0$ (dark yellow "$\diamondsuit$" symbols), displaying the T_c^2 BNC scaling, is the same calculation as in Fig.2 with $\Gamma_0 = 0.10$ and $\Gamma_\pi = 0.05$ but only over $\bar{N}_h \in [0.7, 1]$. Then the three other solid symbols are the calculation results for the region of $\bar{N}_h \in [0.5, 0.7]$ with three different strengths of magnetic order $M(\bar{N}_h)$ of Fig.3(A). The results of Fig.3(B) reveal an interesting behavior; namely, although it is more natural to expect that $\Delta C/T_c$ vs. T_c with a coexisting magnetic order should behave differently from the one without a magnetic order[14], the calculations of Fig.3(B) with a crude phenomenological treatment of the coexisting magnetic and SC orders show that it is quite robust to follow the BNC scaling even with widely different strengths of M. We trace the origin of this surprising result to the fact that the underdoped region (i.e. where $\bar{N}_h$ is near 0.5 and T_c is maximum), when the magnetic order is absent, is the region where the BNC scaling is best obeyed due to the kinematic constraint of the multiband superconductor (see Fig.1(c) and Fig.2). Therefore, even if the magnetic order modifies the pair susceptibility $\chi_{h,e}(M)$ and cuts out a part of DOS from N^0_{tot}, the generic kinematic constraint of the multiband superconductor dominated by $\bar{V}_{inter}$ is still operative.

Summary and Conclusions — We showed that the puzzling BNC scaling relation $\Delta C/T_c \sim T_c^2$[1] observed in a wide range of the FePn/Ch SC compounds[1–9] is a manifestation of the generic property of the multiband superconductor paired by a dominant inter-band pairing potential $V_{inter} > V_{intra}$. The underlying mechanism is the kinematic constraint $\frac{\Delta_h}{\Delta_e} \sim \sqrt{\frac{N_e}{N_h}}$ near T_c, and the subsequent relations of $\Delta C \sim N_h N_e$ and $T_c(\sqrt{N_h N_e})$. A consideration of the non-pair-breaking impurity effect which broadens the quasiparticle spectra near T_c also explains the evolution from the ideal BNC scaling to its strong deviation as found in $Ba_{1-x}K_xFe_2As_2$[10].

Acknowledgement – YB was supported by Grants No. 2013-R1A1A2-057535 funded by the National Research Foundation of Korea. GRS was supported by the US Department of Energy, contract no. DE-FG02-86ER45268.

[1] S. L. Budko, N. Ni, and P. C. Canfield, Phys. Rev. B **79**, 220516 (2009).
[2] J. S. Kim, G. R. Stewart, S. Kasahara, T. Shibauchi, T. Terashima, and Y. Matsuda, J. Phys.: Condens. Matter 23, 222201 (2011).
[3] F. Hardy *et al.*, Phys. Rev. B **81**, 060501(R) (2010); F. Hardy *et al.*, Europhys. Lett. **91**, 47008 (2010).
[4] K. Gofryk *et al.*, Phys. Rev. B 81, 184518 (2010); K. Gofryk, A. B. Vorontsov, I. Vekhter, A. S. Sefat, T. Imai, E. D. Bauer, J. D. Thompson, and F. Ronning, *ibid.* **83**, 064513 (2011).
[5] J. S. Kim, B. D. Faeth, and G. R. Stewart, Phys. Rev. B 86, 054509 (2012).
[6] C. Chaparro *et al.*, Phys. Rev. B **85**, 184525 (2012).
[7] P. Walmsley *et al.*, Phys. Rev. Lett. **110**, 257002 (2013).
[8] S. L. Bud'ko *et al.*, Phys. Rev. B **89**, 014510 (2014).
[9] J. Xing *et al.*, Phys. Rev. B **89**, 140503 (2014).
[10] S. L. Bud'ko, M. Sturza, D. Y. Chung, M. G. Kanatzidis, and P. C. Canfield, Phys. Rev. B 87, 100509 (2013).
[11] V. G. Kogan, Phys. Rev. B 80, 214532 (2009); V. G. Kogan, *ibid.* **81**, 184528 (2010).
[12] A. A. Abrikosov, L. P. Gorkov, and I. E. Dzyaloshinski, *Methods of Quantum Field Theory in Statistical Physics*, (Dover, New York, 1963), Eq.(36.9) in p.306.
[13] In the strong pair-breaking limit ($\Gamma_\pi > T_c$) where $\Delta F \propto -N(0)\frac{\Delta^4}{\Gamma_\pi^2}$ is valid, the behavior of $\Delta(T)$ should also change to $\Delta^2(T) \propto \Gamma_\pi^2(1 - \frac{T}{T_c})$ instead of the BCS behavior $\Delta^2(T) \propto T_c^2(1-\frac{T}{T_c})$. Then the SH jump in this limit becomes $\Delta C/T_c \sim N(0)\frac{\Gamma_\pi^2}{T_c^2}$, quite opposite to the BNC scaling.
[14] M. G. Vavilov, A. V. Chubukov, and A. B. Vorontsov, Phys. Rev. B **84**, 140502(R) (2011); M. G. Vavilov and A. V. Chubukov, *ibid.*, **84**, 214521 (2011).
[15] J. Zaanen, Phys. Rev. B **80**, 212502(R) (2009).
[16] I.I. Mazin, D.J. Singh, M.D. Johannes, M.H. Du, Phys. Rev. Lett. **101**, 057003 (2008); K. Kuroki, S. Onari, R. Arita, H. Usui, Y. Tanaka, H. Kontani, and H. Aoki , *ibid.*, **101**, 087004 (2008).
[17] Y. Bang and H.-Y. Choi, Phys. Rev. B, **78**, 134523 (2008).
[18] Y. Bang, H.-Y. Choi, and H. Won, Phys. Rev. B **79**, 054529 (2009).
[19] For the undoped parent compound $BaFe_2As_2$, our model assumes $\bar{N}_h = \bar{N}_e = 0.5$. For electron doping in $Ba(Fe_{1-x}Co_x)_2As_2$, hole pocket(s) disappears ($\bar{N}_h = 0$) around $x \approx 0.15$. For the hole doping cases, electron pockets(s) disappears ($\bar{N}_e = 0$) in $(Ba_{1-x}K_x)Fe_2As_2$ when $x > 0.7$ but in $(Ba_{1-x}Na_x)Fe_2As_2$ the electron pocket still remains when $x \approx 1$. Therefore, the actual doping "x" and our model doping parameter $\bar{N}_{h,e}$ should be properly rescaled according to the T_c variation vs. doping.
[20] A. A. Abrikosov and L. P. Gorkov, Sov. Phys. JETP **12**, 1243 (1961).
[21] S. Skalski, O. Betbeder-Matibet, and P.R. Weiss, Phys. Rev. **136**, A1500 (1957), see Eq.(5.19).